Accepted Manuscript

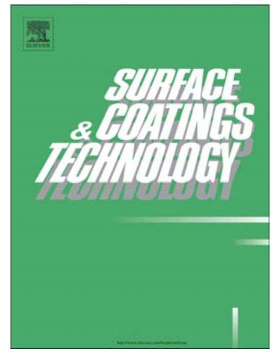

Evolution of structural, mechanical and tribological properties of Ni–P/MWCNT coatings as a function of annealing temperature

Qianzhi Wang, Mauro Callisti, Alberto Miranda, Brian McKay, Ioanna Deligkiozi, Tatjana Kosanovic Milickovic, Alexandros Zoikis-Karathanasis, Kostas Hrissagis, Luca Magagnin, Tomas Polcar

PII: S0257-8972(16)30502-3
DOI: doi: 10.1016/j.surfcoat.2016.06.011
Reference: SCT 21253

To appear in: *Surface & Coatings Technology*

Received date: 7 April 2016
Revised date: 30 May 2016
Accepted date: 5 June 2016

Please cite this article as: Qianzhi Wang, Mauro Callisti, Alberto Miranda, Brian McKay, Ioanna Deligkiozi, Tatjana Kosanovic Milickovic, Alexandros Zoikis-Karathanasis, Kostas Hrissagis, Luca Magagnin, Tomas Polcar, Evolution of structural, mechanical and tribological properties of Ni–P/MWCNT coatings as a function of annealing temperature, *Surface & Coatings Technology* (2016), doi: 10.1016/j.surfcoat.2016.06.011

Evolution of structural, mechanical and tribological properties of Ni-P/MWCNT coatings as a function of annealing temperature

Qianzhi Wang[a*], Mauro Callisti[a], Alberto Miranda[b], Brian McKay[b], Ioanna Deligkiozi[c], Tatjana Kosanovic Milickovic[d], Alexandros Zoikis-Karathanasis[d], Kostas Hrissagis[d], Luca Magagnin[e], Tomas Polcar[a]

[a] National Centre for Advanced Tribology at Southampton, Department of Mechanical Engineering, Faculty of Engineering and the Environment, University of Southampton, Southampton SO17 1BJ, UK

[b] Institute of Materials and Manufacturing, Brunel University, London UB8 3PH, UK

[c] Centre for Technology Research and Innovation, Limassol 3106, Cyprus

[d] Centre for Research and Technology Hellas (CERTH/IRETETH), Trikala GR42100, Greece

[e] Dip. Chimica, Materiali e Ing. Chimica Giulio Natta, Politecnico di Milano, Milano 20131, Italy

Abstract: The structural, mechanical and tribological properties of Ni-P/MWCNT coatings annealed at various temperatures (350-500°C) were investigated using XRD, SEM, nanoindentation and tribometer to determine the optimal annealing temperature for their enhanced tribological properties. The results showed that the annealed coatings comprised a hard Ni_3P phase, and consequently presented a higher hardness (from 7.0±0.3 to 8.2±1.4 GPa) than the as-plated sample (6.0±0.9 GPa). With the annealing temperature increasing from 350 °C to 500 °C, the crystallinity of coating was enhanced with larger crystal grains of Ni and Ni_3P, which led to a decline in hardness (from 8.2 to 7.0 GPa) due to the Hall-Petch effect. Owing to the lubrication effect of H_3PO_4 arising from the tribochemical reaction of Ni_3P with ambient environment, the annealed samples exhibited lower friction coefficients (0.71~0.86) compared to the as-plated coating (0.87). A combination of low surface roughness and the reduction of oxides on wear track contributed to the lowest friction coefficient of Ni-P/MWCNT annealed at 400 °C. However, the decomposition of amorphous carbon in MWCNT over 380 °C produced less dense coatings (for annealing temperatures 400-500 °C), and their incompact structure led to a higher wear rate (2.9-3.0×10^{-5} mm^3/Nm) compared to the as-plated sample (2.4×10^{-5} mm^3/Nm). In contrast, Ni-P/MWCNT

* Corresponding author. Tel.: +44-23-8059-4438.
E-mail address: jxwqz1985@aliyun.com; qz.wang@nuaa.edu.cn

coating annealed at 350 °C (< 380 °C) exhibited a better wear resistance (4.3×10^{-6} mm^3/Nm). Thus, 350 °C was found to be the optimal annealing temperature to lower the friction coefficient and enhance the wear resistance of Ni-P/MWCNT coatings.

Keywords: Nickel-phosphorus; MWCNT; Electrodeposition; Tribology; Annealing.

1. Introduction

Owing to their excellent resistance to both wear and corrosion, electroplated hard chrome coatings are one of the widely used surface treatments in the aerospace, automotive and shipping industries [1-3]. Nevertheless, with a growing awareness on environment protection and human health, researchers are looking for viable alternative to hard chrome coatings to avoid the hazardous Cr^{6+} (a genotoxic carcinogen) in electrolytic baths [4-7].

In order to minimise additional costs for plating industry, researchers have concentrated their attention on Ni-P coatings using existing equipment. Consequently, several studies investigated the influence of pH value [8], surfactant [9], bath parameters [10] and post-treatment [11, 12] in order to optimise the structural and tribological properties of Ni-P coatings. Nevertheless, the low hardness of the as-plated Ni-P coatings (400-500 HV0.025) still stands in its way of a wide application in tribology field, where hardness is deemed as a vital property. Therefore, various reinforcing particles have been introduced into Ni-P coatings to increase their hardness and as a consequence enhance their tribological properties.

Amongst SiC [13], TiN [14], TiO_2 [15], SiO_2 [16, 17], WC [18], Al_2O_3 [19], B_4C [20] and CNT [21-23] reinforcing particles, SiC and MWCNT incorporations demonstrated a greater enhancement in hardness (ΔH>260 HV0.01). Compared with SiC, CNT has shown an extremely high Young's modulus up to 1.0 TPa and a high tensile strength around 60 GPa [24]. Moreover, CNT is expected to provide superior lubrication effect than SiC due to its integrated molecule, in which the carbon atoms are bonded with sp^2 hybrid [24]. For instance, Chen et al. [25] found that Ni/CNT composite coatings exhibited a lower friction coefficient (0.075) than Ni/SiC coatings (0.130). Tu et al. [26, 27] pointed out that MWCNT co-deposition reduced the friction coefficient of Ni-P coatings down to 0.063 compared to 0.124 for SiC reinforced ones. A similar result was also reported in Ref. [28] as listed in Table 1. However, in current literature, only a few studies have focused on the role of heat treatment in determining the tribological properties of Ni-P/MWCNT coatings [23, 25, 27, 29, 30]. More importantly, the coatings in the above studies were all deposited using electroless technique, whilst the chosen interval of annealing temperature was too large (200 °C) to help us understand the tendencies from 200 to 400 °C and from 400 to 600 °C. Thus, it is of paramount importance to study the detailed evolution of the tribological properties for annealed Ni-P/MWCNT coatings with a small interval of temperature, especially for the coatings fabricated by using electrodeposition.

In this present study, electrodeposited Ni-P/MWCNT coatings annealed at four different temperatures (350, 400, 450 and 500 °C) as well as the as-plated coating (50 °C) were compared in order to study the effect of heat treatment on their tribological properties. The correlation between annealing temperature, microstructure, mechanical and tribological properties of Ni-P/MWCNT coatings was subsequently elucidated.

2. Experimental details

2.1 Composite coatings electroplating and annealing

Multi-walled carbon nanotubes (MWCNTs) with 3-15 walls (Inner diameter 2-6 nm and outer diameter 5-20 nm) and length of 1-10 μm were selected as reinforcing particles (supplied by EMFUTUR Technologies). In order to evaluate the quality of MWCNTs, a Renishaw inVia confocal Raman microscope with an excitation energy of 2.54 eV and a Raman shift from 800 to 2000 cm^{-1} was used. In addition, a simultaneous thermogravimetric analysis (TGA) and differential scanning calorimetry (DSC) analysis at a heating rate of 10 ºC/min was conducted in a He atmosphere (40 mL/min) to assess the thermal stability of MWCNTs up to 900 ºC (NETZCH STA 409 PC Luxx). After being dispersed in 10 ml of ethanol in an ultrasonic bath for 2 minutes, two drops of the MWCNTs suspension were pipetted onto a 400 # Cu grid, and then naturally dried under ambient condition prior to the observation by using transmission electron microscope (TEM) operated at 80 kV (JEOL 2100 FEG). To remove surface contaminants on the substrates, the carbon steel plates with dimensions of 4×6 cm^2 were anodized in NaOH (1.25 M) and immersed in HCl (1:8) consecutively. Afterwards, they were covered by galvanic tape (3M 470 Electroplating and Anodizing Vinyl Tape) leaving an exposed area of 4×4 cm^2. Suzuki et al. [31] and Li et al. [32] found that the Ni-P/MWCNT composite coatings with a lower concentration of CNT (0.7% mass) exhibited superior tribological properties. Thus, 1 g/L of MWCNT was loaded into the electrolytic bath in this study to keep a low concentration of MWCNT in Ni-P/MWCNT coatings. The plating electrolyte contained nickel sulphate as nickel source, phosphorous acid as P source and nickel chloride to support the dissolution of Ni-S anode. Based on the hardness and surface roughness (R_a) of Ni-P/MWCNT coatings as a function of current density (5, 10, 15 and 20 $A \cdot dm^{-2}$) in our previous work, Ni-P/MWCNT coating (4.9 wt% P and 60 μm thick) electroplated at 20 $A \cdot dm^{-2}$ is chosen as the subject in this paper. In order to ensure a uniform electrolyte solution, a magnetic stirring at 300 rpm was applied during the entire electroplating process. The deposition parameters for the preparation of the composite coatings are listed in Table 2.

Using an electric furnace, the as-plated Ni-P/MWCNT coatings (50 °C) were annealed at 350, 400, 450 and 500 °C, and hereafter denoted as Ni-P/MWCNT-50, Ni-P/MWCNT-350, Ni-P/MWCNT-400, Ni-P/MWCNT-450 and Ni-P/MWCNT-500. During heat treatment, a constant heating rate of 5 °C/min was maintained until the target temperature was reached. After a holding time of 1 h, samples were cooled naturally to room temperature. In order to remove the surface oxides by heat treatment, all of the specimens were mechanically polished using 0.3 μm Al_2O_3 suspension for 5 minutes.

2.2 Microstructure and mechanical properties of composite coatings

The morphology of the Ni-P/MWCNT coatings after mechanical polishing was observed by scanning electron microscope (SEM) (JEOL-JSM-6500F), and their chemical composition was analyzed by energy dispersive spectroscopy (EDS) equipped on SEM (FEI Quanta 200). By using X-ray diffraction (XRD) with a Cu-K_α radiation (Siemens D-5000), the phase conditions of the as-plated and annealed coatings were characterized within a 2θ range from 20° to 100° at a scanning rate of 5 °/min and a step size of 0.05°. To investigate the mechanical properties of the Ni-P/MWCNT coatings, nanoindentation (Micromaterials) under a penetration depth of 500 nm (<10% of the coatings thickness) was carried out. In order to ensure the reliability of data, 10 nanoindentations were conducted for each coating. The surface roughness (*R*a) of coatings after polishing was measured using a 3D optical microscope (Infinite Focus).

2.3 Evaluation of tribological properties

The friction and wear behavior of Ni-P/MWCNT coatings under ambient condition was evaluated by using a reciprocating tribometer (TE77, Phoenix Tribology, Ltd.). Since the potential application of Ni-P/MWCNT coatings on crankshaft, 52100 steel balls (Ø 6 mm), as a common material for linkage, was selected as counterpart in this study. In order to achieve the friction coefficient within the steady period, which appears after running-in period and before the failure of coatings, the stroke length, frequency and applied load of the tribotest were kept at 10 mm, 5 Hz and 10 N respectively for a duration of 1 hour. All of the tribotests were repeated twice to ensure the reliability of data, with a third test necessary if the relative error of friction coefficient was over 5 %. A 3D optical microscope (Infinite Focus) was subsequently used to analyze the contours of wear tracks. Accordingly, the wear volume of coatings can be determined from the product of cross-section area (A) and wear length (L). In addition, the morphology of wear tracks were observed by SEM (JEOL-JSM-6500F), and their corresponding chemical compositions were analyzed using EDS (Inca Energy 350).

3. Results and discussions

3.1 Characterization of MWCNT and Ni-P/MWCNT composite coatings

The TEM images of MWCNT under different magnifications are shown in Fig.1a and 1b. It is clear that the MWCNTs used in this study are of various diameters as stated in experimental details. The XRD spectrum of MWCNT in Fig.1c demonstrates its common crystallinity whilst the Raman spectrum in Fig.1d indicates the presence of amorphous carbon (a-C) [33]. Consequently, as seen in Fig.2, two endothermic peaks around 420 ºC and 500 ºC in DSC trace are closely associated with the decomposition of a-C. As a result, a sharp weight loss is observed in TGA diagram from 380 °C to 500°C. It is in contrast to pure MWCNT (i.e. without any amorphous carbon), which should remain stable up to 2800 ºC [34].

As seen in Fig.3a, the XRD spectrum of the Ni-P/MWCNT-50 coating exhibits two broad peaks at 44.5° and 97.8°, which are related to Ni (111) and Ni (222) (JCPDS 00-004-0850). However, the crystallinity of Ni is significantly enhanced after annealing, and continues to increase with increasing annealing temperature. In addition, new diffraction peaks (around 42.8°, 43.6°, 60.2°, 74.9° and etc.) are observed in XRD spectra after heat treatment, which were identified as

Ni_3P crystal (JCPDS 01-089-2743) by DIFFRAC.EVA software (Siemens Energy and Automatization, Inc.) . The size evolution of Ni (111) and Ni_3P (231) grains as a function of annealing temperature was calculated according to the Scherrer's equation [35], and the results are presented in Fig.3b. It is obvious that the crystal grains of Ni (111) and Ni_3P (231) grow from 6 nm to 50 nm and from 34 nm to 59 nm, respectively, as the annealing temperature increases. Note that no MWCNT was detected in diffractograms of Ni-P/MWCNT coatings because of a very low incorporation amount (1.9 wt%).

The surface morphology and individual roughness (*R*a) of the Ni-P/MWCNT coatings after polishing are shown in Fig.4. The Ni-P/MWCNT-50 coating exhibits the highest *R*a of 7.9±0.5 μm with obvious agglomeration structure. In contrast, few agglomeration structures are evident in the annealed coatings and the Ni-P/MWCNT-400 coating exhibits the lowest *R*a of 6.7±0.2 μm. This lower asperity has a beneficial effect on its friction behavior, which will be discussed elsewhere (in section 3.3).

3.2 Characterization of mechanical properties

The hardness (H) and reduced elastic modulus (E_r) of each coating were obtained from loading-unloading curves by applying the Oliver and Pharr method [36], whilst the recovery of elasticity (R_e) was calculated via maximum (h_{max}) and residual (h_f) depths. As listed in Table 3, all of the annealed specimens exhibit a higher hardness (7.0±0.3-8.2±1.4 GPa) than the as-plated one (6.0±0.9 GPa) due to the formation of a hard intermetallic Ni_3P crystalline phase [37]. Nevertheless, the increasing grain size of Ni (111) and Ni_3P (231) with increasing temperature leads to a reduction in hardness from 8.2 to 7.0 GPa based on the Hall-Petch effect. Since elastic modulus has an equal role as hardness in determining tribological properties, some researchers have suggested using the ratios of H/E_r and H^3/E_r^2 for tribology prediction, as they are proportional to the resistance to elastic strain and plastic deformation, respectively [38]. Moreover, coatings with a superior R_e should encounter lower plastic deformation. Thus, according to the values in Table 3, the Ni-P/MWCNT-350 coating is expected to present the best tribological performance due to a combination of the highest H/E_r, H^3/E_r^2 and R_e, followed by the Ni-P/MWCNT-400 coating.

3.3 Evaluation of friction

Fig.5 shows the friction behavior of Ni-P/MWCNT coatings as a function of sliding time. It is clear that the friction coefficient of all the samples decreases gradually from its original value to a steady state value after a specific 'running-in' period. Due to a relatively rougher surface with a higher *R*a (Fig.4a&b), the Ni-P/MWCNT-50 and Ni-P/MWCNT-350 coatings encounter a longer 'running-in' period - more time is needed to remove large asperities [39]. In contrast, the Ni-P/MWCNT-450 and Ni-P/MWCNT-500 coatings exhibit a shorter 'running-in' period due to a lower *R*a (Fig.4d&e). Interestingly, the Ni-P/MWCNT-400 coating presents the longest 'running-in' period (around 2100 s) even with the smoothest morphology. In principle, surface quality largely determines the length of the 'running-in' period, but hardness is another important factor that needs to be considered. As listed in Table 3, the Ni-P/MWCNT-400 coating exhibits the highest hardness (8.2 GPa), which contributes to a low rate of asperity removal. As a result, the friction coefficient of Ni-P/MWCNT-400 coating takes more time to reach a steady state; a similar phenomenon was reported in Ref. [37]. Furthermore, it is worth noting that the smoothest morphology of the Ni-P/MWCNT-400 coating contributes to a steady friction behavior during the entire tribotest. In contrast, dramatic fluctuations of the friction coefficient are observed on the friction behavior of the other coatings.

By averaging the friction coefficient attained during steady state, the mean-steady friction coefficient of each coating is illustrated in Fig.6a. Obviously, all of the annealed coatings exhibit a lower friction coefficient (0.71±0.031~0.86±0.042) than the as-plated condition (0.87±0.055). This discrepancy is attributed to the different tribochemical reactions during the tribotest as described below [40]:

$$4Ni + 3O_2 = 2Ni_2O_3 \quad (1)$$

$$\Delta G_f^{298} = -287.6 kJ \cdot mol^{-1}$$

$$2Ni_3P + 7O_2 = 3Ni_2O_3 + P_2O_5 \quad (2)$$

$$\Delta G_f^{298} = -1364.7 kJ \cdot mol^{-1}$$

$$P_2O_5 + 3H_2O = 2H_3PO_4 \quad (3)$$

$$\Delta G_f^{298} = -144.1 kJ \cdot mol^{-1}$$

According to the standard Gibbs free energy [41-43], tribochemical reactions (1-3) can occur spontaneously. Incongruent with the tribochemical reaction of the Ni-P/MWCNT-50 coating (Eq. (1)), the oxidation of Ni_3P in annealed coatings (Eqs. (2) and (3)) generates not only Ni_2O_3 but also P_2O_5, which is extremely unstable in air. Subsequently, the generated P_2O_5 absorbs the moisture from its ambient environment to form orthophosphoric acid (H_3PO_4). It has been reported that, in H_3PO_4 environment, a lubricant gel containing Fe-P-O and electrical double layer effect contributed to a drop in friction coefficient. Hence, all the annealed samples exhibit a lower friction coefficient than the as-plated coating in this study.

It is worth noting that the Ni-P/MWCNT-400 coating exhibits the lowest friction coefficient of 0.71±0.031 amongst the annealed samples. Except for the lubrication effect of H_3PO_4 as mentioned above, there are two reasons contributing to such a outcome. One is the smoothest morphology (*R*a=6.7±0.2 μm), which offers an even contact interface between coatings and balls at the beginning stage of tribotest. This favorable condition has a lasting effect during the whole friction behavior, because a lower *R*a helps obtain a lower mean-steady friction coefficient [44-46]. The other reason is the amount of oxides formed during the tribotest. In principle, the formation of oxides should decrease friction coefficient due to their softness under dry friction condition. However, the adhesion and accumulation of oxides could increase the roughness of wear track, thus leading to a higher friction coefficient due to mechanical interlock. As seen in Fig.7, EDS analyses indicate that the wear track on the Ni-P/MWCNT-400 coating contains the lowest concentration of oxygen (3.6 wt%). Therefore, a lower amount of oxides (Ni_2O_3 and FeO_x) was generated in the wear track resulting in a relatively smoother sliding interface, which contributed to a lower friction.

3.4 Evaluation of wear

Analyzing the coatings wear rate in Fig.6b and the hardness in Table.3, it is found that the wear resistance of Ni-P/MWCNT coatings is not proportional to their hardness. For instance, the coatings annealed at 400, 450 and 500 °C are harder but present higher wear rates (2.9-3.0×10^{-5} mm^3/Nm) than the as-plated condition (2.4×10^{-5} mm^3/Nm). Furthermore, even with the same hardness (8.2 GPa), the Ni-P/MWCNT-350 and Ni-P/MWCNT-400 coatings exhibit a big difference in wear rate with one order of magnitude (4.3×10^{-6} mm^3/Nm and 2.9×10^{-5} mm^3/Nm). These results imply that there is another key factor determining their wear resistance.

According to the TGA and DSC shown in Fig.2, the decomposition of amorphous carbon in MWCNTs takes place around 380 °C. Hence, during the heat treatment, Ni-P/MWCNT-400, Ni-P/MWCNT-450 and Ni-P/MWCNT-500 coatings suffered the decomposition of amorphous carbon, which deteriorated their compact structure. In contrast, only a limited decomposition of amorphous carbon occurred during the annealing at 350 °C, i.e. the Ni-P/MWCNT-350 coating was still compact and dense after annealing. Therefore, the decomposition of amorphous carbon in MWCNT is the key factor significantly limiting the wear resistance of Ni-P/MWCNT coatings. Consequently, Ni-P/MWCNT-400, Ni-P/MWCNT-450 and Ni-P/MWCNT-500 coatings exhibit a higher wear rate than the softer Ni-P/MWCNT-50 coating, whilst Ni-P/MWCNT-350 coating exhibits the lowest value (4.3×10^{-6} mm^3/Nm).

4. Conclusions

Ni-P/MWCNT composite coatings were electroplated on carbon steel plates followed by annealing at various temperatures (350-500 °C). The evolution of their microstructure, mechanical and tribological properties as a function of annealing temperature was investigated. Conclusions are drawn as follows:

(1) With increasing annealing temperature, the crystallinity of Ni in the Ni-P/MWCNT coatings increased, and a Ni_3P phase was formed.

(2) Owing to the presence of the hard Ni_3P phase, annealed samples exhibited a higher hardness (7.0-8.2 GPa) than the as-plated sample (6.0 GPa). However, the increasing grain size led to a drop in hardness from 8.2 GPa to 7.0 GPa due to the Hall-Petch effect.

(3) The Ni-P/MWCNT-400 coating exhibited the lowest friction coefficient of 0.71±0.03 due to a combination of the lubricious effect of H_3PO_4 from tribochemical reaction, a smoother original contact surface and fewer oxides formed on the wear track.

(4) The decomposition of amorphous carbon in MWCNTs (T > 380 °C), rather than the hardness, was the key factor to the wear resistance of Ni-P/MWCNT coatings. Thus, the Ni-P/MWCNT coatings annealed at 400, 450 and 500 °C exhibited a poor wear resistance (wear rate: $2.9\text{-}3.0\times10^{-5}$ mm^3/Nm) while the Ni-P/MWCNT coating annealed at 350 °C presented the strongest wear resistance (wear rate: 4.3×10^{-6} mm^3/Nm).

Acknowledgement

This work has been supported by the collaborative research project Hardalt (Grant No. 606110) funded by the EU's seventh framework programme.

References

[1] V.S. Protsenko, F.I. Danilov, V.O. Gordiienko, S.C. Kwon, M. Kim, J.Y. Lee, Electrodeposition of hard nanocrystalline chrome from aqueous sulfate trivalent chromium bath. Thin Solid Films 520 (2011) 380-383.

[2] K. Ranjbar, M. Sababi, Failure assessment of the hard chrome coated rotors in the downhole drilling motors. Eng. Fail. Anal.20 (2012) 147-155.

[3] M. Srivastava, C. Anandan, V.K.W. Grips, Ni-Mo-Co ternary alloy as a replacement for hard chrome. Appl. Surf. Sci. 285 (2013) 167-174.

[4] Risk & Policy Analysts Limited, Environmental Risk Reduction Strategy and Analysis of Advantages and Drawbacks for Hexavalent Chromium, Norfolk, 2005.

[5] B. Sonntag, V. Sundaram, Substitution of Cr (VI)-containing coatings by the European automobile industry. Indian Surf. Finish. 1 (2004) 15-26.

[6] M.D. Cohen, M. Costa, Chromium, in: M. Lippmann, Environmental Toxicants: Human Exposures and Their Health Effects, Second ed., Wiley, New York, 2000, pp. 173-191.

[7] U.S. Department of Health and Human Services, Agency for Toxic Substances and Disease Registry, Toxicological Profile for Chromium, Atlanta, Georgia, 2012.

[8] X.W. Zhou, H.M. Jin, L.N. Zhang, Influence of pH value on microstructure and thermal stability of Ni-P electroless coating prepared in acidic condition. Chinese Chem. Lett. 20 (2009) 845-848.

[9] R. Elansezhian, B. Ramamoorthy, P. K. Nair, Effect of surfactants on the mechanical properties of electroless (Ni-P) coating. Surf. Coat. Technol. 203 (2008) 709-712.

[10] B. Panja, P. Sahoo, Wear behavior of electroless Ni-P coatings in brine solution and optimization of coating parameters. Procedia Technol. 14 (2014) 173-180.

[11] M. Novak, D. Vojtech, P. Novak, T. Vitu, Tribological properties of heat-treated electroless Ni-P coatings on AZ91 alloy. Appl. Surf. Sci. 257 (2011) 9982-9985.

[12] J.D. Lin, C.L. Kuo, Effects of hydrogen plasma treatment on microstructure evolution and

electrical conductivity of electroless Ni-P coatings on polyimide and glass substrates. Surf. Coat. Technol. 209 (2012) 80-89.

[13] S.S. Zhang, K.J. Han, L. Cheng, The effect of SiC particles added in electroless Ni-P plating solution on the properties of composite coatings. Surf. Coat. Technol. 202 (2008) 2807-2812.

[14] I.R. Mafi, C. Dehghanian, Studying the effects of the addition of TiN nanoparticles to Ni-P electroless coatings. Appl. Surf. Sci. 258 (2011) 1876-1880.

[15] S.M.A. Shibli, V.S. Dilimon, Effect of phosphorous content and TiO_2-reinforcement on Ni-P electroless plates for hydrogen evolution reaction. Int. J. Hydrogen Energy 32 (2007) 1694-1700.

[16] Y. Hazan, D. Zimmermann, M. Zgraggen, S. Roos, C. Aneziris, H. Bollier, P. Fehr, T. Graule, Homogeneous electroless Ni-P/SiO_2 nanocomposite coatings with improved wear resistance and modified wear behaviour. Surf. Coat. Technol. 204 (2010) 3464-3470.

[17] M. Islam, M.R. Azhar, N. Fredj, T.D. Burleigh, O.R. Oloyede, A.A. Almajid, S.I. Shah, Influence of SiO_2 nanoparticles on hardness and corrosion resistance of electroless Ni-P coatings. Surf. Coat. Technol. 261 (2015) 141-148.

[18] Z.A. Hamid, S.A.E. Badry, A.A. Aal, Electroless deposition and characterization of Ni-P-WC composite alloys. Surf. Coat. Technol. 201 (2007) 5948-5953.

[19] S. Karthikeyan, B. Ramamoorthy, Effect of reducing agent and nano Al_2O_3 particles on the properties ofelectroless Ni-P coating. Appl. Surf. Sci. 307 (2014) 654-660.

[20] M.E. Hosseinabadi, K.A. Dorcheh, S.M.M. Vaghefi, Wear behavior of electroless Ni-P-B_4C composite coatings. Wear 260 (2006) 123-127.

[21] A. Zarebidaki, S.R. Allahkaram, Effect of surfactant on the fabrication and characterization of Ni-P-CNT composite coatings. J. Alloys Compd. 509 (2011) 1836-1840.

[22] M. Alishahi, S.M. Monirvaghefi, A. Saatchi, S.M. Hosseini, The effect of carbon nanotubes on the corrosion and tribological behavior of electroless Ni-P-CNT composite coating. Appl. Surf. Sci. 258 (2012) 2439-2446.

[23] Z. Yang, H. Xu, Y.L. Shi, M.K. Li, Y. Huang, H.L. Li, The fabrication and corrosion behavior of electroless Ni-P-carbon nanotube composite coatings. Mater. Res. Bull. 40 (2005) 1001-1009.

[24] R. Sudhakar, V.T. Venkatesha, Electrodeposition of Zn-Ni multiwalled carbon nanotube nanocomposites and their properties. Ind. Eng. Chem. Res. 52 (2013) 6422-6429.

[25] X.H. Chen, C.S. Chen, H.N. Xiao, H.B. Liu, L.P. Zhou, S.L. Li, G. Zhang, Dry friction and

wear characteristics of nickel/carbon nanotube electroless composite deposits. Tribol. Int. 39 (2006) 22-28.
[26] W.X. Chen, J.P. Tu, Z.D. Xu, W.L. Chen, X.B. Zhang, D.H. Cheng, Tribological properties of Ni-P-multi-walled carbon nanotubes electroless composite coating. Mater. Lett. 57 (2003) 1256-1260.
[27] W.X. Chen, J.P. Tu, H.Y. Gan, Z.D. Xu, Q.G. Wang, J.Y. Lee, Z.L. Liu, X.B. Zhang, Electroless preparation and tribological properties of Ni-P-carbon nanotube composite coatings under lubricated condition. Surf. Coat. Technol. 160 (2002) 68-73.
[28] C.S. Chen, X.H. Chen, Z. Yang, W.H. Li, L.S. Xu, B. Yi, Effect of multi-walled carbon nanotubes as reinforced fibres on tribological behaviour of Ni-P electroless coatings. Diamond Relat. Mater. 15 (2006) 151-156.
[29] W.X. Chen, J.P. Tu, L.Y. Wang, H.Y. Gan, Z.D. Xu, X.B. Zhang, Tribological application of carbon nanotubes in a metal-based composite coating and composites. Carbon 41 (2003) 215-222.
[30] Q. Shi, W.C. Sun, J. Gao, Y. Wang, M.M. Tian, Effects of Heat Treatment on Mechanical Properties of Ni-P-CNT Composite Coating. Mater. Sci. Forum 817(1) (2015) 1662-9752.
[31] Y. Suzuki, S. Arai, M. Endob, Electrodeposition of Ni-P alloy-multiwalled carbon nanotube composite films. J. Electrochem. Soc. 157 (2010) D50-D53.
[32] Z.H. Li, X.Q. Wang, M. Wang, F.F. Wang, H.L. Ge, Preparation and tribological properties of the carbon nanotubes-Ni-P composite coating. Tribol. Int. 39 (2006) 953-957.
[33] R.A. DiLeo, B.J. Landi, R.P. Raffaelle, Purity assessment of multiwalled carbon nanotubes by Raman spectroscopy. J. Appl. Phys. 101 (2007) 064307 1-5.
[34] P. G. Collins, P. Avouris, Nanotubes for electronics, Sci. Am. 283 (2000) 62-69.
[35] P. Scherrer, N.G.W. Gottingen, Math-Pys. Kl. 2 (1918) 96-100.
[36] W.C. Oliver, G.M. Pharr, An improved technique for determining hardness and elastic modulus using load and displacement sensing indentation experiments. J. Mater. Res. 7 (1992) 1564-1583.
[37] D. Nava, C.E. Dávalos, A. Martínez-Hernández, F. Manríquez, Y. Meas, R. Ortega-Borges, J.J. Pérez-Bueno, G. Trejo, Effects of heat treatment on the tribological and corrosion properties of electrodeposited Ni-P alloys. Int. J. Electrochem. Sci. 8 (2013) 2670-2681.
[38] N.A. Sakharova, J.V. Fernandes, M.C. Oliveira, J.M. Antunes, Influence of ductile interlayers on mechanical behaviour of hard coatings under depth-sensing indentation: a numerical study on

TiAlN. J. Mater. Sci. 45 (2010) 3812-3823.

[39] Q.Z. Wang, F. Zhou, X.D. Ding, Z.F. Zhou, C.D. Wang, W.J. Zhang, L. K-Y. Li, S-T. Lee, Microstructure and water-lubricated friction and wear properties of CrN(C) coatings with different carbon contents. Appl. Surf. Sci. 268 (2013) 579-587.

[40] Q.Z. Wang, M. Callisti, J. Greer, B. McKay, T.K. Milickovic, A. Zoikis-Karathanasis, I. Deligkiozi, T. Polcar, Effect of annealing temperature on microstructure, mechanical and tribological properties of nano-SiC reinforced Ni-P coatings. Wear 356-357 (2016) 86-93.

[41] H.G. Zhu, Y.L. Ai, J.L. Li, J. Min, D. Chu, J. Zhao, J. Chen, In situ fabrication of α-Al_2O_3 and Ni_2Al_3 reinforced aluminum matrix composites in an Al-Ni_2O_3 system. Adv. Powder Technol. 22 (2011) 629-633.

[42] M.H. Sandstrom, D. Bostrom, Determination of standard Gibbs free energy of formation for $CaKPO_4$, $CaK_4(PO_4)_2$, $CaK_2P_2O_7$, and $Ca_{10}K(PO_4)_7$ from solid-state e.m.f. measurements using yttria stabilised zirconia as solid electrolyte. J. Chem. Thermodynamics 40 (2008) 40-46.

[43] Thermodynamic Properties, in: J.A. Dean, Lange's Handbook of Chemistry, Fifteenth ed., Mcgraw-hill, Inc., New York, 1998, pp. 545-702.

[44] R.G. Lu, H.D. Zhang, Y. Mitsuya, K. Fukuzawa, S. Itoh, Influence of surface roughness and coating on the friction properties of nanometer-thick liquid lubricant films. Wear 319 (2014) 56-61.

[45] M.L. Rahaman, L.C. Zhang, M. Liu, W.D. Liu, Surface roughness effect on the friction and wear of bulk metallic glasses. Wear 332-333 (2015) 1231-1237.

[46] H.I. Dawood, K.S. Mohammed, A. Rahmat, M.B. Uday, The influence of the surface roughness on the microstructures and mechanical properties of 6061 aluminium alloy using friction stir welding. Surf. Coat. Technol. 270 (2015) 272-283.

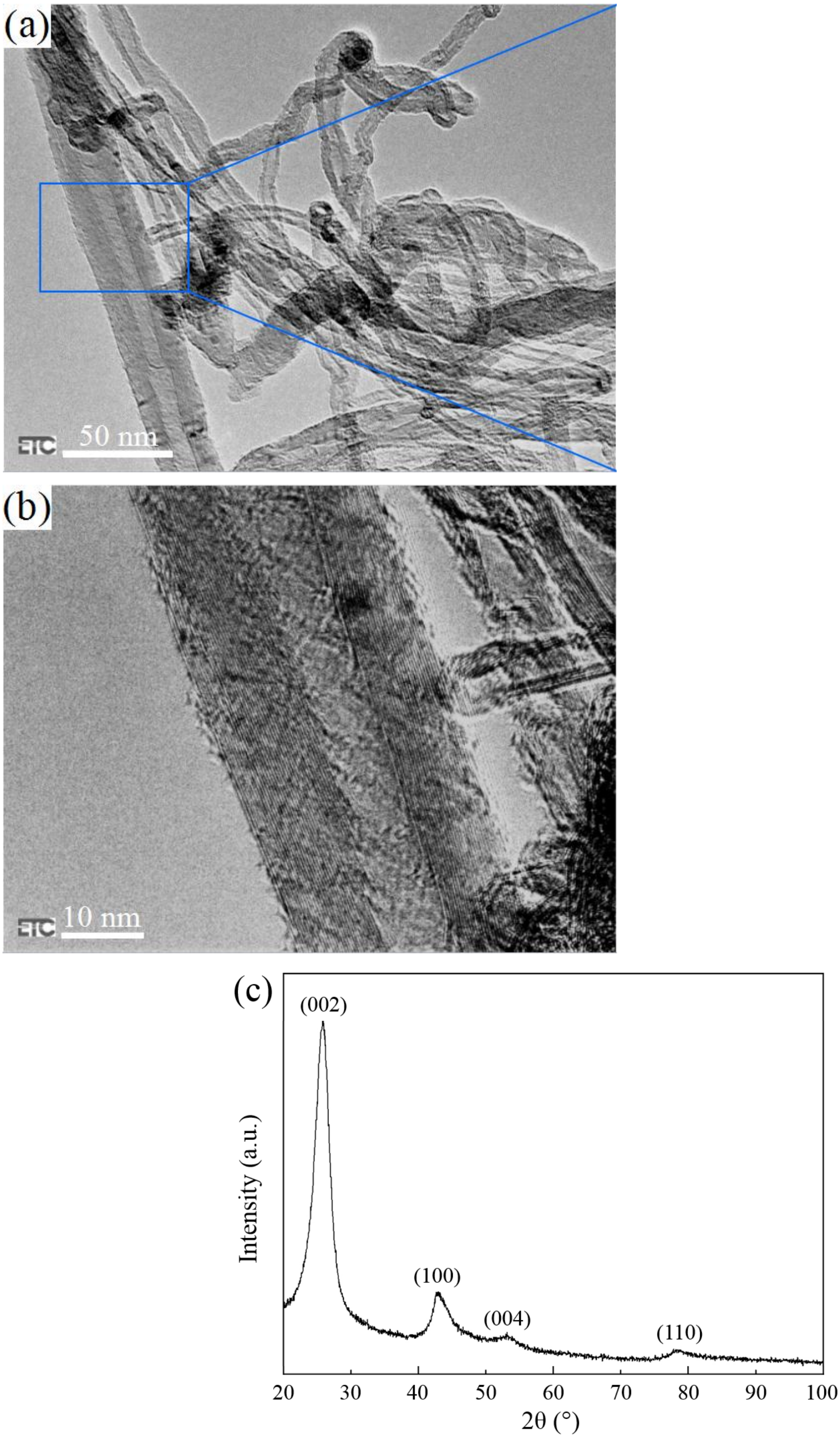
(a)
50 nm
(b)
10 nm
(c)
(002)
(100)
(004)
(110)
Intensity (a.u.)
2θ (°)
20
30
40
50
60
70
80
90
100

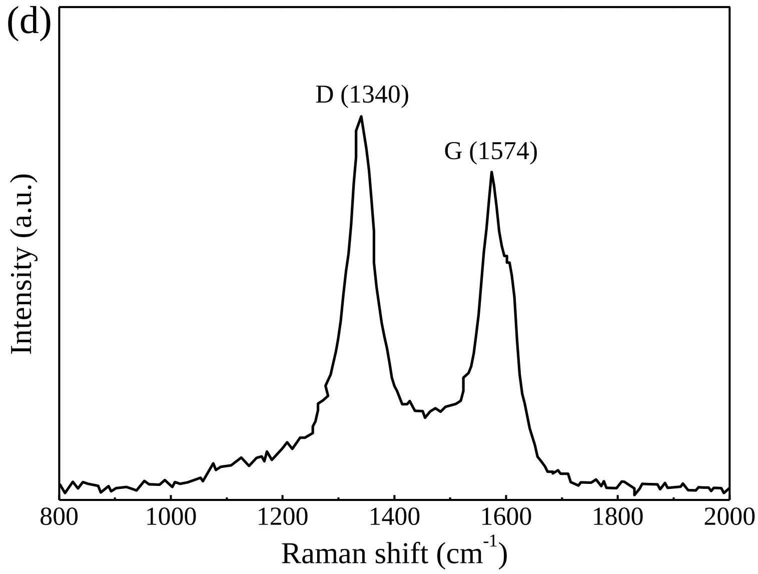

Fig.1 (a) (b) TEM images (c) XRD and (d) Raman spectra of MWCNT

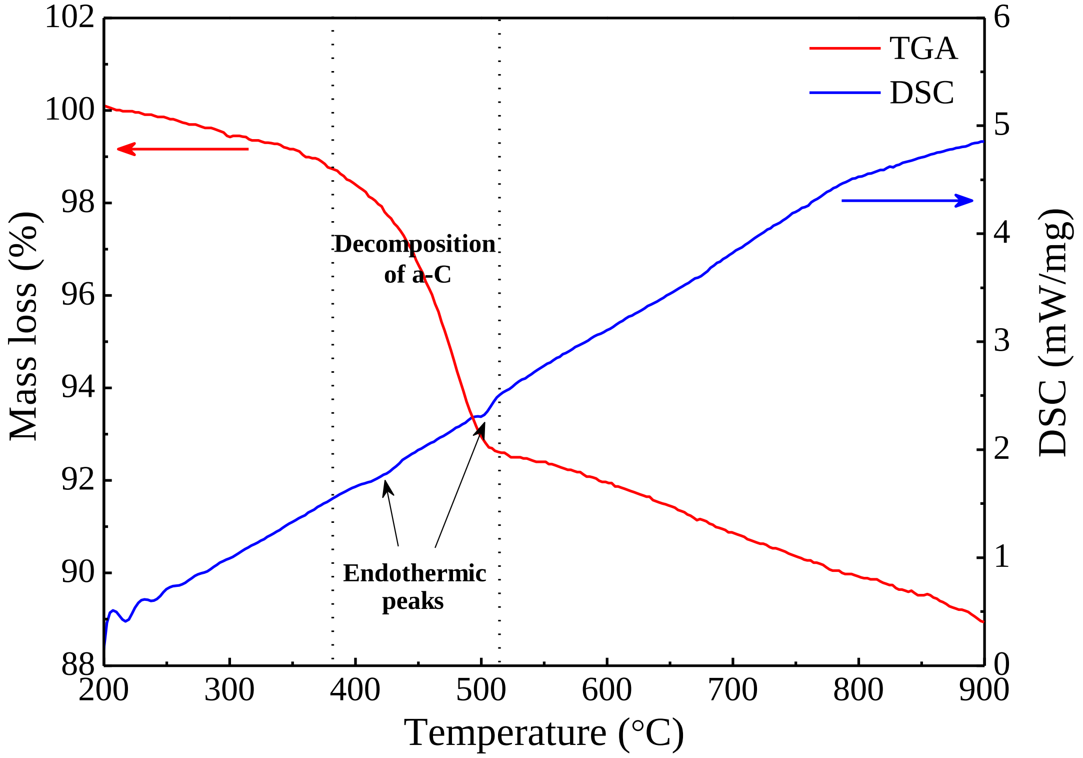

Fig.2 Differential scanning calorimetry (DSC) and **thermogravimetric analysis** (TGA) of MWCNT under a He atmosphere

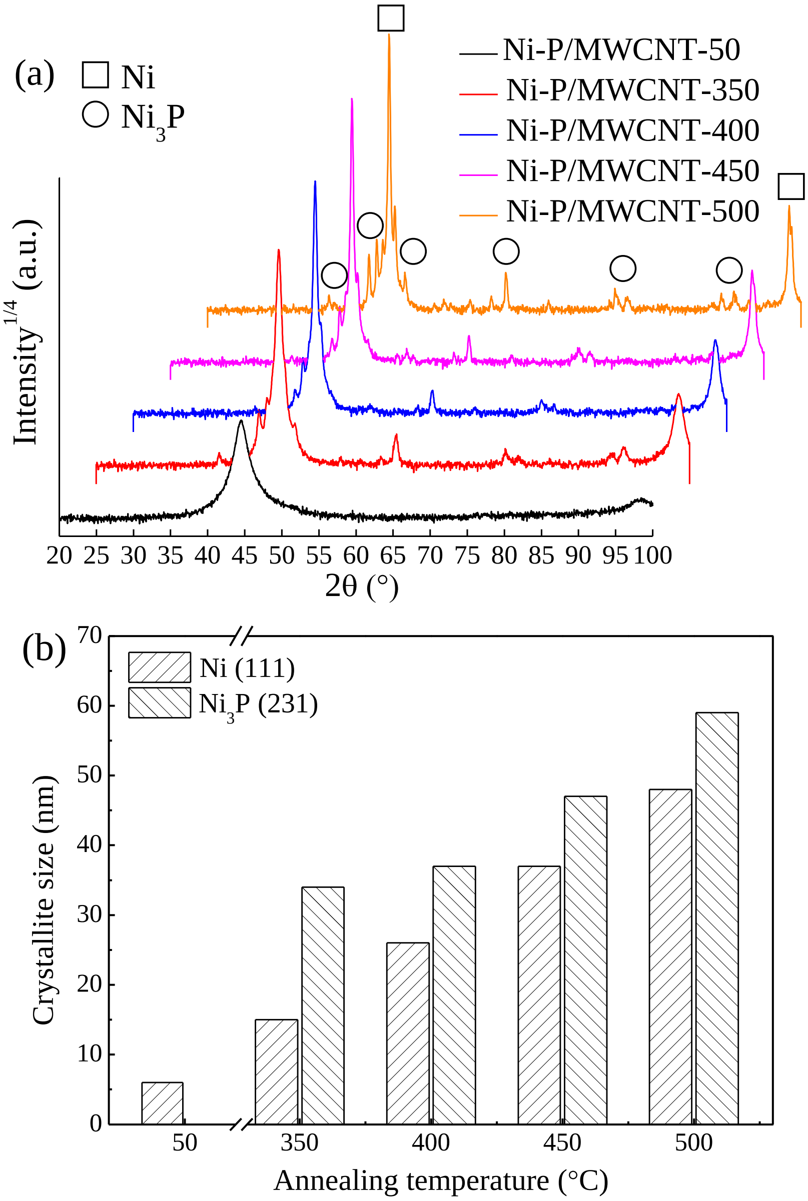

Fig.3 (a) XRD spectra and (b) crystalline sizes of Ni (111) and Ni_3P (231) of Ni-P/MWCNT coatings annealed at different temperatures

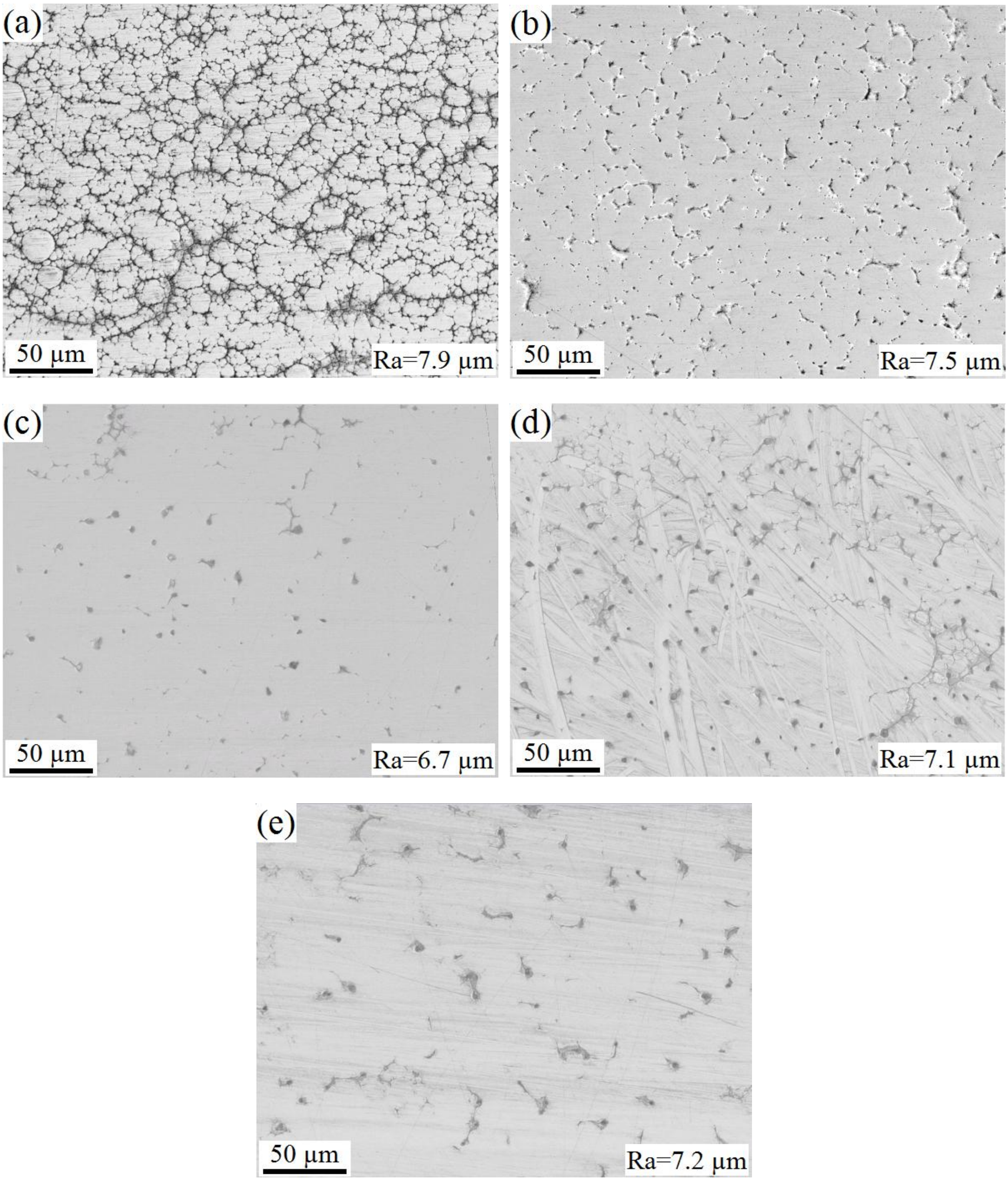

Fig.4 Morphology of the polished (a) Ni-P/MWCNT-50 (b) Ni-P/MWCNT-350 (c) Ni-P/MWCNT-400 (d) Ni-P/MWCNT-450 and (e) Ni-P/MWCNT-500 coatings

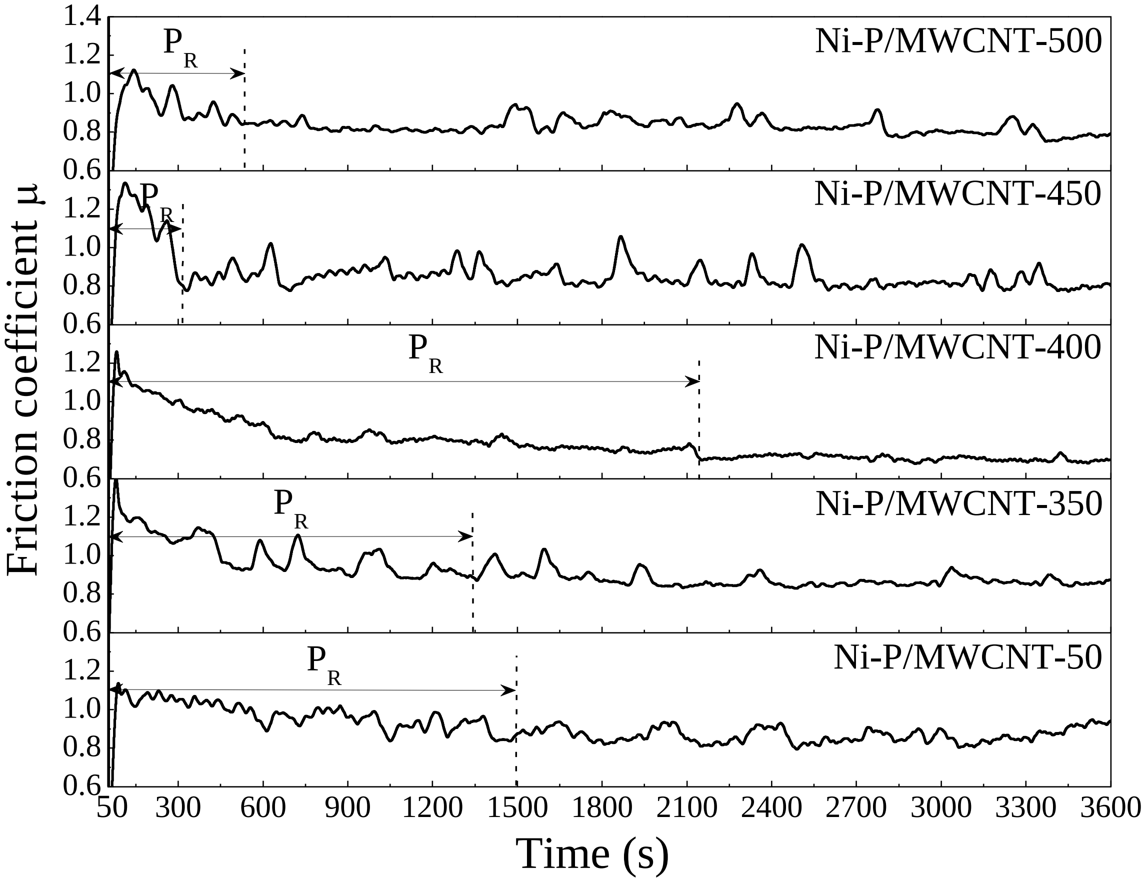

Fig.5 Friction behavior of Ni-P/MWCNT coatings annealed at different temperatures sliding against 52100 balls

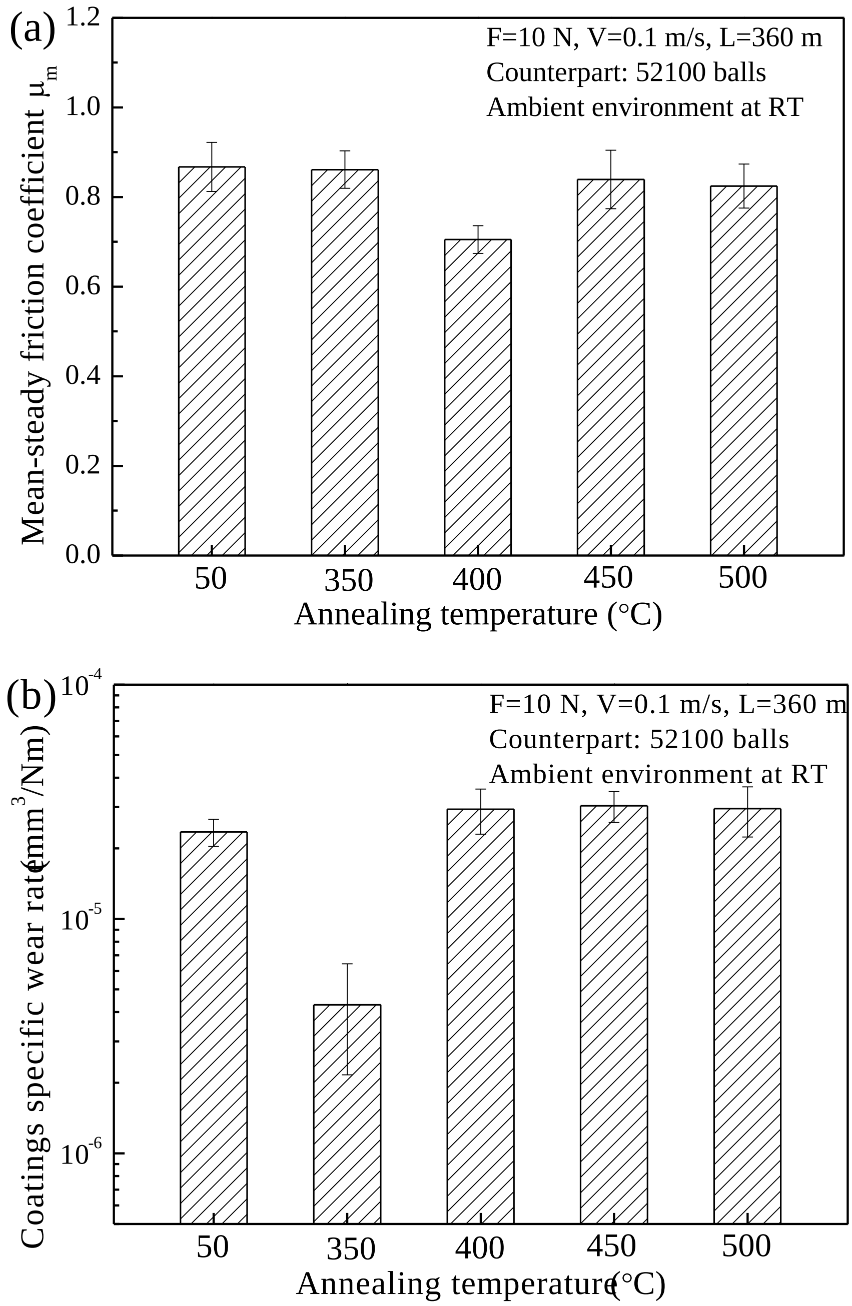

Fig.6 (a) Mean-steady friction coefficient and (b) wear rate of Ni-P/MWCNT coatings annealed at different temperatures

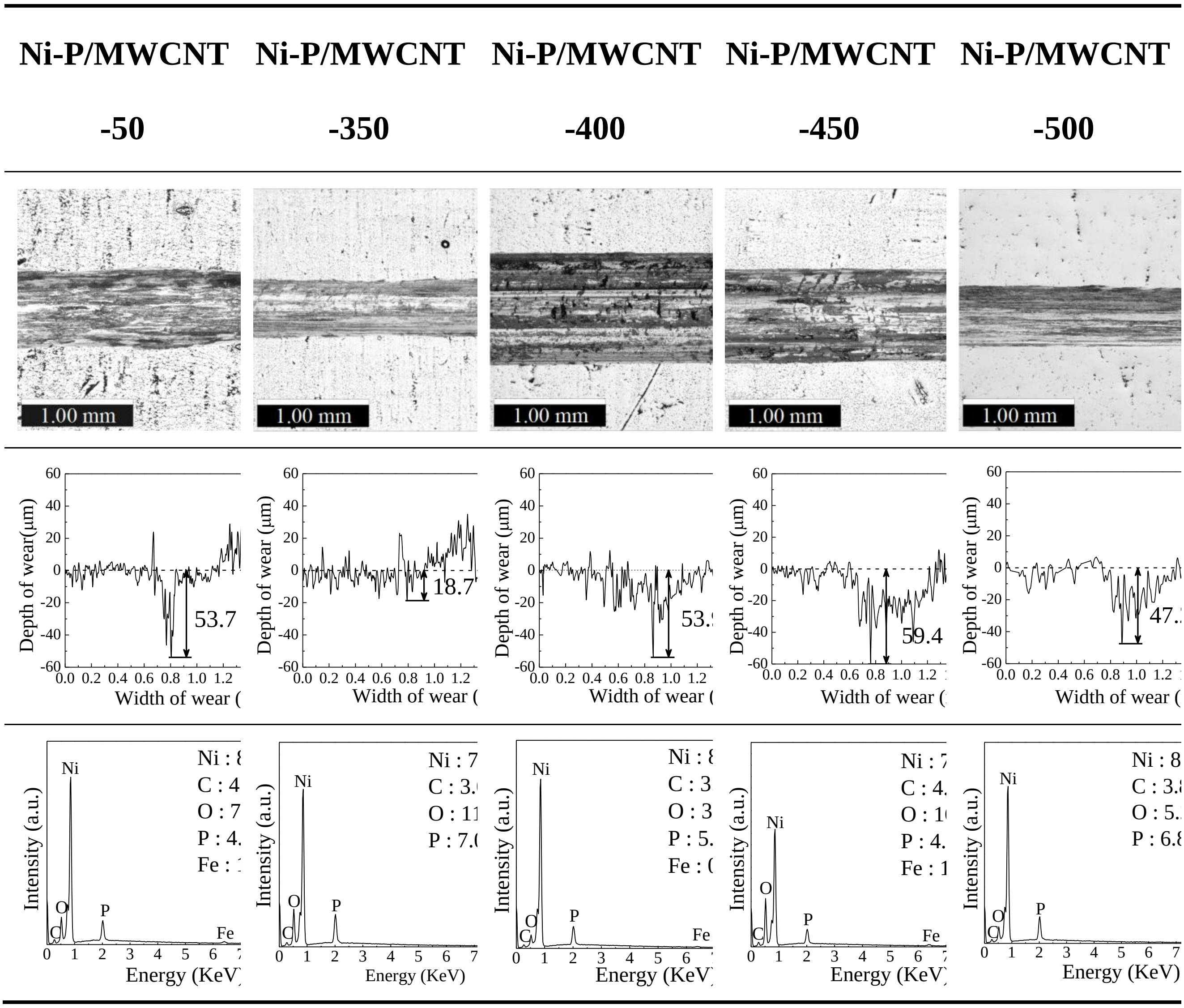

Fig.7 Morphology, contours and the corresponding EDS analyses of wear tracks on Ni-P/MWCNT coatings annealed at different temperatures

Table 1 Mechanical and tribological properties of Ni and Ni-P coatings alloying with SiC and CNT particles

Reference	**Coatings**	**Particles**	**Hardness**	**Friction coefficient**	**Wear depth or mass loss**
Chen et al. [25]	Ni	SiC	725 HV0.025	0.130	11.2 μm
		CNT	865 HV0.025	0.075	6.6 μm
Tu et al. [26, 27]	Ni-P	SiC	550 HV0.05	0.124	8.5 mg
		MWCNT	520 HV0.05	0.063	6.2 mg
Chen et al. [28]	Ni-P	SiC	725 HV0.025	0.147	5.7 mg
		MWCNT	946 HV0.025	0.122	3.0 mg

Table 2 Electro-deposition conditions of Ni-P/MWCNT coatings

Temperature	50±2 ^{o}C
pH	1±0.2
MWCNT load	1 g/L
Current density	20 Adm^{-2}
Substrate	Steel platelet
Anode	Nickel (S)

Table 3 Mechanical properties of Ni-P/MWCNT coatings at different annealing temperatures

Coatings	***H*** **(GPa)**	$\boldsymbol{E_r}$ **(GPa)**	$\boldsymbol{H/E_r}$	$\boldsymbol{H^3/E_r^2}$ **(GPa)**	$\boldsymbol{R_e}$ **(%)**
Ni-P/MWCNT-50	6.0±0.9	156±6	0.038	0.009	14.7±1.8
Ni-P/MWCNT-350	8.2±1.4	190±14	0.043	0.015	16.6±1.9
Ni-P/MWCNT-400	8.2±0.6	209±7	0.039	0.013	15.2±0.9
Ni-P/MWCNT-450	7.4±0.3	224±14	0.033	0.008	12.8±1.0
Ni-P/MWCNT-500	7.0±0.3	213±4	0.033	0.008	12.6±0.6

Highlights

- Annealing improved the crystallinity of Ni and promoted the formation of Ni_3P.
- All annealed coatings exhibited a higher hardness since the formation of Ni_3P.
- H_3PO_4 from tribochemical reaction of Ni_3P decreased friction of annealed coatings.
- 350 °C was the optimal annealing temperature to enhance tribological properties.
- Decomposition of amorphous carbon in MWCNT was the key factor to wear resistance.